

Surface potential analysis of AlN/GaN heterostructures by electrochemical capacitance-voltage measurements

C. Pietzka,^{1,a)} G. Li,² M. Alomari,¹ H. Xing,² D. Jena,² and E. Kohn¹

¹*Institute of Electron Devices and Circuits, Ulm University, 89069 Ulm, Germany*

²*Department of Electrical Engineering, University of Notre Dame, Notre Dame, Indiana 46556, USA*

(Received 1 August 2012; accepted 10 September 2012; published online 8 October 2012)

AlN/n⁺-GaN heterostructure samples with AlN barrier layer thickness between 1 nm and 4 nm have been analyzed by electrochemical capacitance-voltage measurements with a semiconductor-electrolyte contact to estimate the surface potential of this heterostructure. The combination of using a semiconductor-electrolyte interface for characterization and using an n⁺-doped GaN buffer layer enabled the extraction of the surface potential from the full range of data between the two flatband conditions, flatband in the AlN barrier and flatband in the GaN buffer. Such analysis is otherwise difficult to obtain due to the tunneling restriction. In the present case of an AlN/GaN heterostructure, the analysis leads to a surface potential of ~ 1.9 eV, independent of the AlN barrier layer thickness. © 2012 American Institute of Physics. [<http://dx.doi.org/10.1063/1.4757932>]

INTRODUCTION

The AlN/GaN heterostructure is an attractive material system for high power/high frequency FET devices due to the high polarization difference between the AlN barrier and the GaN buffer layer. Two-dimensional electron gas (2DEG) densities of up to $6 \times 10^{13} \text{ cm}^{-2}$ can be reached and planar enhancement mode devices have been realized.¹⁻³ One open point in the understanding of these heterostructures is the analysis of the surface barrier characteristics of the free surface and here especially the correlation between surface potential and surface traps, which are thought to act as surface donors and are therefore also thought to be the source of the electrons in the 2DEG.⁴ The surface potential (or surface barrier height) is given by the position of the surface Fermi level, relatively to the conduction band minimum.

Apart from physical surface characterization methods like angle-resolved x-ray photoelectron spectroscopy⁵ or Kelvin force microscopy,⁶ the analysis of the surface barrier characteristics is usually performed either by Hall or by Schottky diode measurements. However, Hall measurements are restricted to barrier layer thicknesses where the 2DEG is not completely depleted by the surface potential and may thus be difficult to apply for enhancement mode devices, if the surface potential of the free surface does not deviate essentially from that of the Schottky contact. The analysis of Schottky diodes becomes inadequate in the case of thin barrier layers, like in the case of AlN/GaN heterostructures, and under forward bias due to tunneling across the barrier. Besides, the Schottky barrier may be different than the barrier on the free AlN surface.

A relatively large number of studies to determine the surface potential in dependence of the barrier layer thickness have been performed for the case of AlGaIn/GaN heterostructures. For the case of an Al content of 34%, originally a single trap level and a pinned surface potential of 1.65 eV

below the conduction band minimum was proposed,⁴ but recent studies indicated that the trap level might be distributed in energy, also depending on the Al content in the AlGaIn barrier and on the surface processing treatment employed, like oxidation or plasma treatments.⁵⁻⁸ These differences might be partially explained by surface donors of different density and energy distribution.⁵ In the case of lattice-matched InAlN/GaN heterostructures grown by metal-organic chemical vapor deposition (MOCVD), a constant and relatively low surface potential of ~ 0.6 - 0.8 eV has been extracted.^{9,10} For the case of AlN/GaN heterostructures, no detailed data are available so far up to our knowledge. Here it is important to note that AlN barrier layers of high quality can only be grown up to a thickness of 4-6 nm due to the large lattice constant mismatch to GaN. Therefore, the analysis of the dependence of the surface potential on the barrier layer thickness is only reasonable in a small range of thin barriers.

In this work, we have analyzed AlN/n⁺-GaN heterostructures by electrochemical capacitance-voltage measurements. The electrolyte-semiconductor contact suppresses tunneling across the interface (within the potential window of water dissociation), the n⁺ doped GaN bulk provides a back-contact and therefore allows the analysis also below pinch-off of the 2DEG. The measurements have been performed in a water-based solution, and the surface is therefore expected to be oxygen-terminated, similar to the case of the technically treated surface during device processing. The method of analysis shown here is especially suited for thin barriers of only a few nm designed for enhancement mode of FET operation.

EXPERIMENTAL

The AlN/n⁺-GaIn heterostructures were grown by molecular beam epitaxy (MBE) on sapphire substrates and semi-insulating GaN buffer layers in a Veeco Gen 930 system. The gas flux was $F_{Ga} = 2.27 \times 10^{-7}$ Torr, the RF power $P \approx 240$ W, and the growth temperature $T \approx 630$ °C.

^{a)}Electronic mail: carsten.pietzka@uni-ulm.de.

The doping concentration in the 90 nm thick n-type GaN layers was $\sim 9 \times 10^{19} \text{ cm}^{-3}$, as confirmed by electrochemical capacitance-voltage measurements of a reference sample without AlN barrier layer (see below). The thickness of the nominally undoped AlN barrier layer was varied between 1.0 nm and 4.0 nm. A schematic cross-section of the heterostructures is depicted in Fig. 1(a). The surface roughness of the samples (RMS value) measured by atomic force microscopy was about 0.3 nm (see Fig. 1(b)). No pits were observed.

For the electrochemical measurements, the heterostructure samples were mounted on a copper holder, contacted using silver paste and passivated with a polytetrafluoroethylene (PTFE)-based adhesive tape with a perforated opening of 1 mm in diameter, which determined the area of the heterostructure electrode exposed to the electrolyte. The surface was therefore not exposed to any thermal or plasma treatment. However, even the exposure to air or electrolyte might affect the surface barrier characteristics. The free surface should therefore be considered as a “technical” surface.

The electrochemical measurements were performed in a standard three-electrode glass cell with a platinum counter and a saturated calomel reference electrode (SCE) in 0.1 M KCl solution ($\text{pH} \approx 6$) using a PARSTAT 273 potentiostat. The corresponding measurement setup is schematically shown in Fig. 2. The current across the AlN/GaN

heterostructure–electrolyte interface (by means of cyclic voltammetry) or the corresponding interface capacitance (by means of capacitance-voltage measurements) is recorded as a function of the potential difference between the sample and the reference electrode. The current flows to the Pt counter electrode, whereas there is no DC current across the reference electrode. This three-electrode system ensures that the measurements are not affected by the characteristics of the counter electrode–electrolyte interface. All measurements were performed at room temperature in the dark. One important point in the analysis is the equilibrium, i.e., the electrode potential versus reference when no external bias is applied. This open-circuit potential was measured to be $\sim +0.1 \text{ V}$ vs. SCE for the case of 0.1 M KCl electrolyte. All electrode potentials in the following will be related to this value and therefore correspond to the externally applied bias. More positive potentials correspond to depletion of the n-type channel, and more negative potentials correspond to accumulation.

The experimental results were compared with simulations of the AlN/GaN heterostructures using a numerical Schrödinger-Poisson solver (Silvaco[®]), taking into account the polarization discontinuity between AlN and GaN of $6 \times 10^{13} \text{ cm}^{-2}$ and a doping concentration of $9 \times 10^{19} \text{ cm}^{-3}$ (which determines the position of the Fermi level in the n⁺-doped GaN bulk).

RESULTS AND DISCUSSION

Flatband conditions in polar heterostructures

To determine the surface potential of doped bulk semiconductors from capacitance-voltage measurements, usually the flatband voltage (or flatband potential) is measured. However, in the case of a polar III-nitride heterostructure, there are two different flatband conditions. Flatband in the AlN barrier layer occurs under an applied forward bias, where the full 2DEG density corresponding to the

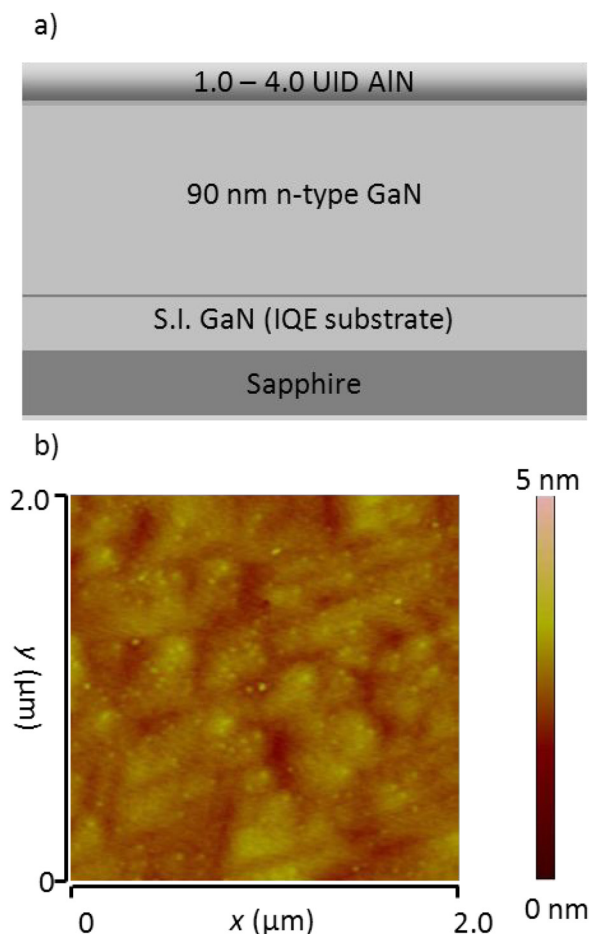


FIG. 1. (a) Schematic cross section of the analyzed layer structures. (b) AFM image of a structure with a 1 nm AlN barrier layer, showing a roughness of 0.4 nm RMS.

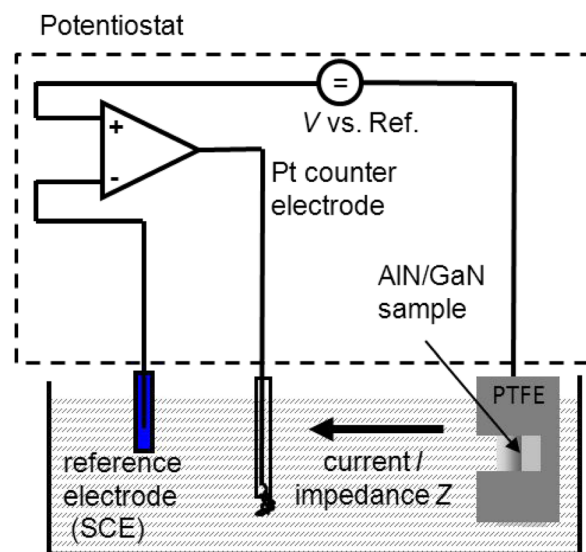


FIG. 2. Experimental setup used for the electrochemical characterization, including a schematic realization of the potentiostat. The three-electrode system eliminates possible effects due to the counter electrode/electrolyte interface.

polarization discontinuity is reached. In this case, the 2DEG and the ionized surface trap counteract and compensate the internal polarization field in the barrier.¹¹ On the other hand, flatband in the n^+ -doped GaN bulk appears when the 2DEG is fully depleted. A higher depletion voltage will result in depletion of the doped GaN bulk, like in the case of doped bulk semiconductors.^{12–14} The potential window for the measurement is that of water dissociation (see Fig. 3). Thus, as already mentioned, the method is especially suited for thin barrier heterostructures which are otherwise difficult to analyze. With the analysis described above, both flatband conditions have been analyzed, which is not possible with Hall or Schottky diode measurements.

Characterization of the heterostructures

Fig. 3 shows the results of a cyclic voltammetry measurement (which records the current across the semiconductor-electrolyte interface for the case of a cyclic potential scan between the onset potentials for hydrogen and oxygen evolution) for the case of a barrier layer thickness of 2 nm. All other samples (with and without different AlN barrier layer thicknesses) showed similar characteristics. The potential window of water dissociation, which is limited by hydrogen evolution and negative and oxygen evolution at positive potentials, is slightly below 3 V, similar to that of other III-nitrides.^{10,13} Within this window, the current is determined by charging and discharging of the interface capacitance, and electrochemical measurements of the heterostructure are possible without strong anodic oxidation or cathodic etching. The hysteresis-like characteristics of hydrogen and oxygen evolution currents might be explained by slow adsorption and desorption of intermediate products formed during the reactions.

Fig. 4(a) shows the capacitance-voltage measurements (Mott-Schottky plots) of a GaN reference sample without AlN barrier, revealing a doping concentration of $9 \times 10^{19} \text{ cm}^{-3}$. In this case, only one flatband conditions exists. At this potential, the capacitance is determined by the electrochemical double layer capacitance, which is related to the adsorption of ions on the AlN-electrolyte interface. The double layer capacitance was taken to be $\sim 10 \mu\text{F}/\text{cm}^2$ and potential-independent, similar to previous studies.^{10,12} The corresponding applied

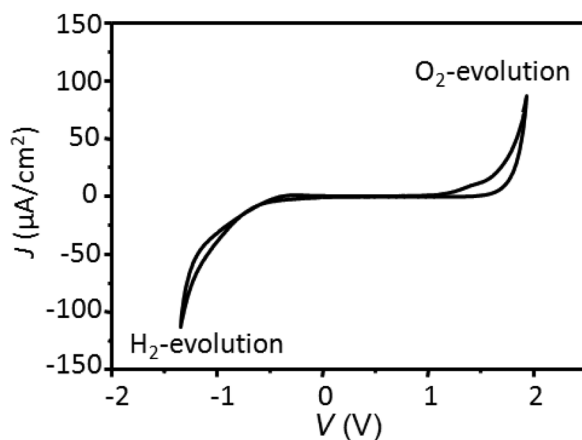


FIG. 3. Cyclic voltammetry for an AlN/GaN heterostructure sample with 1 nm barrier layer thickness in 0.1 M KCl measured with 50 mV/s scan rate. The potential window is ~ 2.5 V with low background currents.

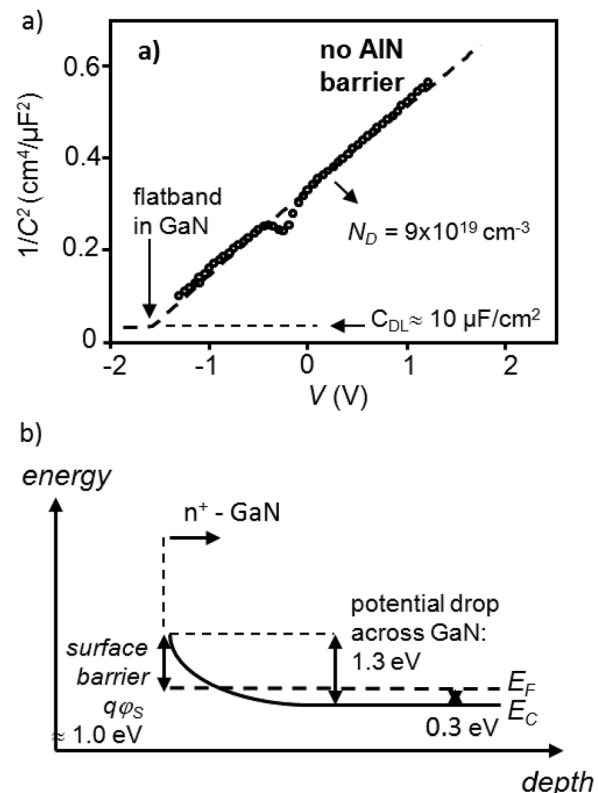


FIG. 4. (a) Results of capacitance-voltage measurements in 0.1 M KCl at $f = 80$ Hz. The deviation of measurements and fit around -0.2 V is most likely related to surface processes. (b) Corresponding band diagram. The Fermi level in the n^+ -GaN lies inside the conduction band.

flatband potential $V_{FB,appl} = -1.6$ V partially drops across the double layer capacitance (ΔV_{DL}) and partially across the depletion layer capacitance (ΔV_{SC}) in the semiconductor in series. The potential drop across the GaN can be calculated by

$$\Delta V_{SC} = \frac{C_{DL}}{C_{DL} + C_{SC}} \times V_{FB,appl}, \quad (1)$$

where $C_{SC} \approx 2.3 \mu\text{F}/\text{cm}^2$ is the calculated depletion layer capacitance under no applied bias. This calculation results in a potential drop across the semiconductor of 1.2–1.3 V and a surface potential of about 1.0 eV, considering that the Fermi level in the GaN bulk lies within the conduction band (see Fig. 4(b)), as calculated by the Schrödinger-Poisson simulation tool. This value for the surface potential of GaN is similar to that obtained by Kelvin force microscopy, although also significantly lower surface potentials have been observed for highly doped GaN.^{15,16} A possible explanation for the higher surface potential in our case could be that even in the absence of any additional surface treatment, the exposure of the surface to atmosphere or to the electrolyte can lead to the formation of a thin native oxide layer and therefore affect the surface potential, as stated before. However, the extracted surface potential of 1.0 eV for an “air-exposed” GaN surface is still reasonable, considering also that this technique has already been successfully used for the analysis of other doped semiconductors.^{12–14}

Fig. 5 shows the results of capacitance-voltage measurements (Mott-Schottky plots) measured at $f = 80$ Hz for the

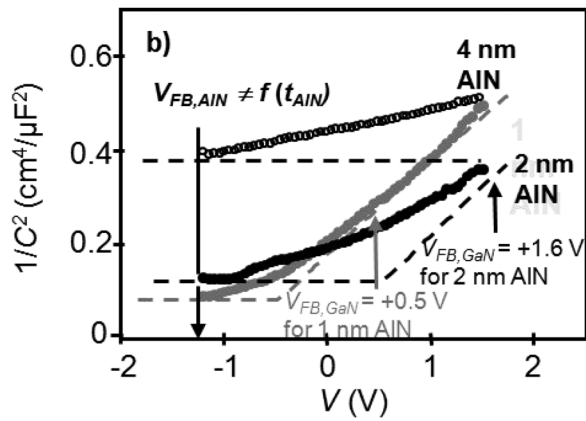


FIG. 5. Results of the capacitance-voltage measurements in 0.1 M KCl for the AlN/n⁺-GaN-heterostructures with three different barrier layer thicknesses. The dashed lines show two-step approximations for the measured data.

cases of 1 nm, 2 nm, and 4 nm barrier layer thickness. The dashed lines show two-step approximations for the measured data: At negative potentials corresponding to full accumulation of the 2DEG, the capacitance is constant and equal to the series connection of the barrier layer and the electrochemical double layer capacitance. The double layer capacitance was again taken to be $\sim 10 \mu\text{F}/\text{cm}^2$. At positive potentials, the slope in the Mott-Schottky plot corresponds to the doping concentration of $9 \times 10^{19} \text{cm}^{-3}$, as recorded for the case of the reference sample without AlN barrier.

The main challenge in interpreting the measurement results is now the extraction of the potentials for flatband in the AlN barrier and the GaN bulk, respectively. These potentials were taken from the potential points where the measurement data start to deviate from the two-step approximation (not taking the 2DEG into account) and are listed in Table I. Coming from highly negative potentials (full 2DEG developed), fit and measurement start to deviate at -1.2 V , which can be explained by the onset of partial depletion of the 2DEG with more positive applied potentials. This value is taken to be the potential for flatband in the barrier $V_{\text{FB,AlN}}$ and is (at least in first approximation) independent of the barrier thickness. In the same way, the potential where fit and measurement data again coincide can be taken as the flatband potential in the GaN buffer $V_{\text{FB,GaN}}$. The value clearly depends on the barrier layer thickness. In the case of a 4 nm barrier, this potential is already outside the measurement window. In summary, the measurements indicate that flatband in the AlN barrier is reached at a potential of -1.2 V independent on the barrier thickness, while the potential

TABLE I. Extracted potentials for flatband condition in the AlN barrier and in the GaN buffer layer, respectively. The surface barrier $q\phi_B$ calculated from these values is $\sim 1.9 \text{ eV}$ and independent on the barrier layer thickness (see also band diagrams in Fig. 6).

AlN barrier thickness (nm)	$V_{\text{FB,AlN}}$ (V)	$V_{\text{FB,GaN}}$ (V)	$q\phi_B$ (eV)
No AlN barrier	...	-1.6	1.0
1.0	-1.2	$+0.5$	1.9
2.0	-1.2	$+1.6$	1.9
4.0	-1.2	$>+2.0$	1.8

required for flatband in the GaN buffer increases with barrier layer thickness.

Band diagrams under both flatband conditions and under equilibrium

The extracted flatband potentials allow the construction of the band diagrams under both flatband conditions and under equilibrium. The two extreme possible scenarios would be a completely unpinned and a fully pinned surface. In the first case, the band diagram under zero applied bias would show a slope within the AlN barrier layer independent on the barrier layer thickness and therefore always the same 2DEG density. This would result in a linear increase of the surface potential with barrier layer thickness. In case of a fully pinned surface potential, the slope across the AlN barrier and the 2DEG density at zero bias would depend on the AlN layer thickness. The third possibility is the case of a surface donor distributed in energy, leading to a variation of the surface potential in a certain range.

Figure 6(a) depicts the case of flatband in the AlN barrier for the present case. Starting on the GaN side of the heterostructure, the difference between Fermi level and conduction band minimum is determined by the doping concentration to $\sim 0.3 \text{ eV}$. In the same way, the depth of the potential well at the AlN/GaN interface is given by the maximum 2DEG density to $\sim 1.1 \text{ eV}$ (both calculated using the Schrödinger-Poisson simulation tool), taking into account the full development of the 2DEG under this flatband condition. Since the 2DEG and the ionized surface charge fully compensate the internal polarization field in the AlN barrier, the net slope across the barrier becomes zero, and the surface potential can be calculated as the sum of the measured flatband voltage and the part of the conduction band discontinuity at the AlN/GaN interface, which is above the (quasi-)Fermi level in the GaN bulk. Taking a conduction band discontinuity of $\sim 1.8 \text{ eV}$,^{17–19} the analysis results in a surface potential of 1.9 eV independent on the barrier layer thickness (see Fig. 6(a)), since the potential for flatband in the AlN barrier was measured to be the same for all three barrier thicknesses (see Fig. 5).

A similar analysis can be performed under the condition of flatband in the GaN bulk, as shown in Fig. 6(b). Here one has to take into account that the slope across the AlN barrier corresponds now to the full polarization field, which is $\sim 0.9 \text{ V/nm}$ for a fixed polarization charge corresponding to $6 \times 10^{13} \text{ cm}^{-2}$.^{17,19} Taking the measured values for $V_{\text{FB,GaN}}$ into account (at least for the cases of 1 nm and 2 nm), the analysis results again in a value close to 1.9 eV . Figure 6(b) shows that the 4 nm barrier would require a flatband potential of $\sim 3.2 \text{ eV}$, which is outside of the available measurement range (see Figs. 3 and 5). All results are summarized in Table I.

The obtained results allow also the construction of the band diagrams under no applied bias, as shown in Fig. 6(c). Since the surface potential is independent on the barrier layer thickness, the slope across the AlN barrier decreases with increasing thickness. This means a higher 2DEG density for larger barrier layer thicknesses.

One can also imagine what should to be expected for the case of a completely unpinned surface potential. As stated

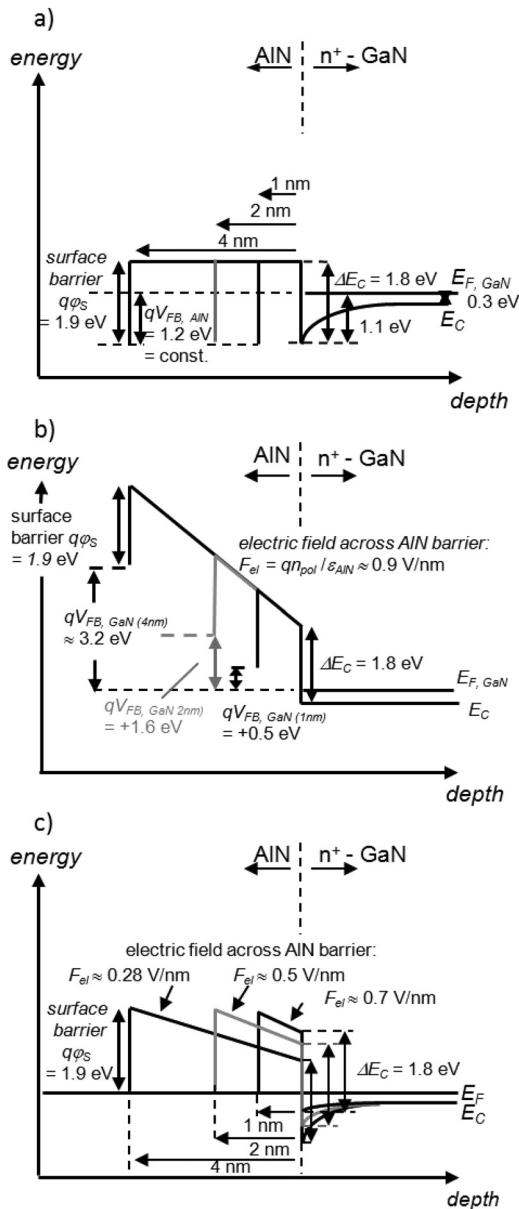


FIG. 6. Energy band diagrams for the heterostructure samples under three different conditions, as extracted from the measurements: (a) flatband in the AlN barrier at an applied potential $V_{FB,AlN}$, (b) flatband in the n^+ GaN buffer at an applied potential $V_{FB,GaN}$, (c) under equilibrium (no applied potential). The analysis gives a surface potential of 1.9 eV independent on the barrier thickness.

before, this would result in a 2DEG density at zero bias which would be independent on the AlN barrier thickness. In this case, the voltage required for flatband in the AlN barrier would increase linearly with increasing barrier layer thickness, since the 2DEG would have to be accumulated across a decreasing capacitance. However, this was not observed in our experiments.

The physical or chemical nature of the surface trap corresponding to the surface potential of 1.9 eV has not been attempted to identify yet. The surface trap might be related to surface oxide groups, since the samples have been exposed to air and have been measured in a water based solution. One important aspect is the density of the surface

traps which determine the surface potential. The simulations show that the band diagram in Fig. 6(c) can be explained by a trap density equal to or larger than the polarization charge discontinuity of $6 \times 10^{13} \text{ cm}^{-2}$ between AlN and GaN. A surface trap density of exactly $6 \times 10^{13} \text{ cm}^{-2}$ would imply that the trap is a direct consequence of the polarization itself, as proposed for the case of InAlN/GaN heterostructures.⁹ Unfortunately, the number of experiments is still too limited to distinguish between the two possibilities. The trap is energetically located 1.9 eV below the conduction band minimum at the AlN surface.

CONCLUSION

AlN/GaN heterostructures with barrier layer thicknesses between 1.0 nm and 4 nm have been analyzed by electrochemical capacitance-voltage measurements in order to estimate the surface potential. This method, together with n^+ -doping of the GaN buffer, allowed analyzing two different flatband potentials, flatband in the AlN barrier and flatband in the GaN buffer. This is not possible with Hall measurements or the analysis of metal Schottky diodes. The results indicate a surface potential of $\sim 1.9 \text{ eV}$, which is to the first order independent of the barrier layer thickness.

- ¹F. Medjdoub, M. Zegaoui, D. Ducatteaux, N. Rolland, and P. A. Rolland, *IEEE Electron Device Lett.* **32**, 874–876 (2011).
- ²C. Y. Chang, S. J. Pearton, C. F. Lo, F. Ren, I. I. Kravchenko, A. M. Dabiran, A. M. Wowchak, B. Cui, and P. P. Chow, *Appl. Phys. Lett.* **94**, 263505 (2009).
- ³T. Zimmermann, D. Deen, J. Simon, P. Fay, D. Jena, and H. G. Xing, *IEEE Electron Device Lett.* **29**, 661–664 (2008).
- ⁴J. R. Ibbetson, P. T. Fini, K. D. Ness, S. P. DenBaars, J. S. Speck, and U. K. Mishra, *Appl. Phys. Lett.* **77**, 250 (2000).
- ⁵M. Hishagiwaki, S. Chowdhury, B. L. Swenson, and U. K. Mishra, *Appl. Phys. Lett.* **97**, 222104 (2010).
- ⁶G. Koley, H.-Y. Cha, J. Hwang, W. J. Schaff, L. F. Eastman, and M. G. Spencer, *J. Appl. Phys.* **96**, 4253–4262 (2004).
- ⁷G. Li, Y. Cao, H. G. Xing, and D. Jena, *Appl. Phys. Lett.* **97**, 222110 (2010).
- ⁸M. Hishagiwaki, S. Chowdhury, M.-S. Miao, B. L. Swenson, C. G. van de Walle, and U. K. Mishra, *J. Appl. Phys.* **108**, 063719 (2010).
- ⁹F. Medjdoub, M. Alomari, J.-F. Carlin, M. Gonschorek, E. Feltin, M. A. Py, N. Grandjean, and E. Kohn, *IEEE Electron Device Lett.* **29**, 422–425 (2008).
- ¹⁰C. Pietzka, A. Denisenko, M. Alomari, F. Medjdoub, J.-F. Carlin, E. Feltin, N. Grandjean, and E. Kohn, *J. Electron. Mater.* **37**, 616–623 (2008).
- ¹¹Y. Lv, Z. Lin, L. Meng, Y. Yu, C. Luang, Z. Cao, H. Chen, B. Sun, and Z. Wang, *Appl. Phys. Lett.* **99**, 123504 (2011).
- ¹²A. Denisenko, C. Pietzka, A. Romanyuk, H. El-Hajj, and E. Kohn, *J. Appl. Phys.* **103**, 014904 (2008).
- ¹³A. Denisenko, C. Pietzka, A. Chuvilin, U. Kaiser, H. Lu, W. J. Schaff, and E. Kohn, *J. Appl. Phys.* **105**, 033702 (2009).
- ¹⁴R. E. Jones, K. M. Yu, S. X. Li, W. Walukiewicz, J. W. Ager, E. E. Haller, H. Lu, and W. J. Schaff, *Phys. Rev. Lett.* **96**, 125505 (2006).
- ¹⁵K. Köhler, J. Wiegert, H. P. Menner, M. Maier, and L. Kirste, *J. Appl. Phys.* **103**, 023706 (2008).
- ¹⁶S. Barbet, R. Aubry, M. A. Di Forte-Poisson, J. C. Jacquet, D. Deresmes, T. Melin, and D. Theron, *Appl. Phys. Lett.* **93**, 212107 (2008).
- ¹⁷O. Ambacher, M. Eickhoff, A. Link, M. Hermann, M. Stutzmann, F. Bernardini, V. Fiorentini, Y. Smorchkova, J. Speck, U. Mishra, W. J. Schaff, V. Tilak, and L. F. Eastman, *Phys. Status Solidi C* **0**, 1878–1906 (2003).
- ¹⁸Y. Cao and D. Jena, *Appl. Phys. Lett.* **90**, 182112 (2007).
- ¹⁹M. Tchernycheva, L. Nevou, L. Doyennette, F. H. Juliene, E. Warde, F. Guillot, E. Monroy, E. Bellet-Amralic, T. Remmele, and F. Albrecht, *Phys. Rev. B* **73**, 125347 (2006).